SSC22-III-09

SCIENCE CONOPS FOR APPLICATION OF SPORT MISSION DATA TO STUDY LARGE (~1000KM) IONOSPHERIC PLASMA DEPLETIONS

Linda Habash Krause, Shelia Nash-Stevenson, Stephen Clanton
NASA Marshall Space Flight Center
Huntsville, AL
1.256.961.7367
Linda.H.Krause@nasa.gov

Rebecca L. Bishop
The Aerospace Corporation
El Segundo, CA

Charles M. Swenson
Utah State University
Logan, UT

Joaquim E. R. Costa, Marcelo Banik de Pádua
Instituto Nacional de Pesquisas Espaciais (INPE)
Sao Jose dos Campos, Brazil

Marco A. Ridenti, Luis Loures, Lidia Shibuya, Jonas Sousa Santos, Jayr de Amorim Filho, Ana Paula Schuch, Sophia Rodrigues Laranja
Instituto Tecnológico de Aeronáutica (ITA)
São José dos Campos, Brazil

Guan Le, Todd Bonalsky
NASA Goddard Space Flight Center
Greenbelt, MD

Rod A. Heelis, Mark W Mankey
University of Texas, Dallas
Dallas, TX

ABSTRACT

The Scintillation Prediction Observations Research Task (SPORT) mission is a single 6U CubeSat space weather satellite planned for an October 2022 launch into an ISS-like orbit. The primary purpose of the SPORT mission is to determine the longitudinal effects on equatorial plasma bubble (EPB) growth resulting from the offset dipole magnetic field of the Earth. By combining field and plasma measurements from SPORT with other low-altitude (i.e., alt < 1000 km) spacecraft, it is possible to investigate large-scale (> 1000 km) EPB structures. The types of investigation made possible by measurements from SPORT and other contemporaneous missions include 1) dynamics of depleted magnetic flux tubes; 2) dynamics of field-aligned EPB expansion versus propagation speed; 3) EPB vertical extent; and 4) EPB temporal evolution. To support these investigation types, the respective modes of conjunctions are: 1) simultaneous intersection of a magnetic flux tube; 2) intersection of magnetic flux tube separated in time; 3) Simultaneous Latitude/Longitude position conjunction; and 4) Non-simultaneous latitude/longitude position conjunction. This paper will summarize the SPORT satellite and data used for Science CONOPS to accomplish these objectives.

INTRODUCTION AND BACKGROUND

The Scintillation Prediction Observations Research Task (SPORT) is a focused investigation on the conditions under which ionospheric variability develops at low latitudes near the equator and leads to scintillations that compromises transmission of RF signals. The SPORT 6U CubeSat mission was proposed

to the Heliophysics Division at NASA HQ under the Heliophysics Technology and Instrument Development for Science program within ROSES, announcement number NNH16ZDA001N-HTIDS, and selected for funding in 2017. It is an international joint partnership with NASA Marshal Space Flight Center, the Brazilian Space Agency (AEB), Brazilian Instituto Nacional de Pesquisas Espaciais (INPE), Brazilian Instituto Tecnológico de Aeronáutica, (ITA), University of Texas Dallas (UTD), The Aerospace Corporation (TAC), NASA Goddard Space Flight Center (GSFC), and the Utah State University (USU) Center for Space Engineering. The United State partners are providing the flight instruments and the launch to orbit; the Brazilian partners are contributing the spacecraft, observatory integration & test, ground observation networks, and mission operations & data management.

The SPORT mission will make progress on the very compelling but difficult problem of understanding preconditions leading to equatorial plasma bubbles. These ionospheric structures have been observed for decades. They are the primary source of radar reflections in the equatorial F-region ionosphere and cause strong scintillations on radio signals passing through them. The relationships between background ionospheric conditions and the irregularity regions, which may influence their growth to high altitudes are poorly understood. SPORT will address two specific questions about these phenomena: (1) What is the state of the ionosphere that gives rise to the growth of plasma bubbles that extend into and above the F-peak at different longitudes? (2) How are plasma irregularities at satellite altitudes related to the radio scintillations observed passing through these regions? To answer these questions, the SPORT mission will collect data sets (instrument data and spacecraft ancillary data) that will be processed to meet the Science Measurement Requirements identified in Table 1.

SPORT MISSION DESCRIPTION

The SPORT spacecraft (S/C), including the bus and the complement of science instruments, is visualized in Figure 1. The S/C is designed to be 3-axis stabilized, with the +z surface (mechanical coordinates) facing into the ram. The pointing fidelity is to within 5° (1σ) to accommodate the operational requirements of the science instruments (Table 1). The primary science objectives require the science instruments to make measurements on-orbit from 1700 until 0200 local time, more precisely described as when the ascending or descending orbit nodes cross the Brazil's geographic equator within the geographic local time bracket.

The EMBRACE Space Weather Center in Brazil will house and maintain data servers to ingest SPORT data within 30 minutes of the satellite passage over two ground stations, one each located in Cuiabá-MT and Cachoeira Paulista-SP, Brazil. Once the data are converted from Level 0 to Level 2 and validated by the instrument providers, they will be made available to the public using the EMBRACE data warehouse portals.

The SPORT instruments accomplish the measurement objectives traced to the science objectives. The following subsections provide relevant details on the instruments, their data, and plans for application of the data.

USU Space Weather Probes (SWP)

The USU Space Weather Probes consist of a Sweeping Langmuir Probe (SLP), Electric Field Probe (EFP), and Sweeping Impedance Probe (SIP). The electric field probe (EFP) is used to measure only one component of both DC and AC electric fields for identifying disturbed regions of the ionosphere. It is an implementation of the double-probe class of in-situ electric field instruments that have been used for decades to observe electric fields in the space environment. It operates by making measurements of the potential difference between two separate conductive sensors immersed in the plasma that are electrically isolated from the spacecraft

electronics. The SLP consists of a 1-mm diameter cylindrical needle that is 60 mm long and deployed away from the spacecraft. The SLP operating in the ion saturation region is used to determine high-resolution ion density measurements (while minimizing spacecraft charging) based on accurate knowledge of the spacecraft speed and the probe ram cross-section area. Temperature is determined by periodically sweeping in a triangle fashion. SIP is used to determine the absolute electron density, irrespective of the payload charging, by monitoring the changing impedance of a short cylindrical probe excited over a range of RF frequencies. The data collected is used to understand the state of ionosphere and nature of the density structures observed.

Compact Total Electron Content Sensor (CTECS)

The Aerospace Corporation provided Compact Total Electron Content Sensor (CTECS) is a GPS Radio Occultation (GPSRO) instrument. It consists of a commercial-off-the-shelf receiver (NovAtel OEM628) with modified software, a custom designed antenna and RF front-end circuit. GPSRO sensors provide two types of measurements: Line-of-sight (LOS) and radio occultation (RO). The GPS constellation satellites transmit signals in the L-band that are received by the SPORT CTECS. CTECS will measure the pseudorange, phase, and the signal-to-noise ratio (SNR)

of both the GPS L1 (1575.42 MHz) and L2 (1227.6 MHz) signals. These measurements are then used to calculate the integrated electron density along the RO signal path. This is referred to as slant Total Electron

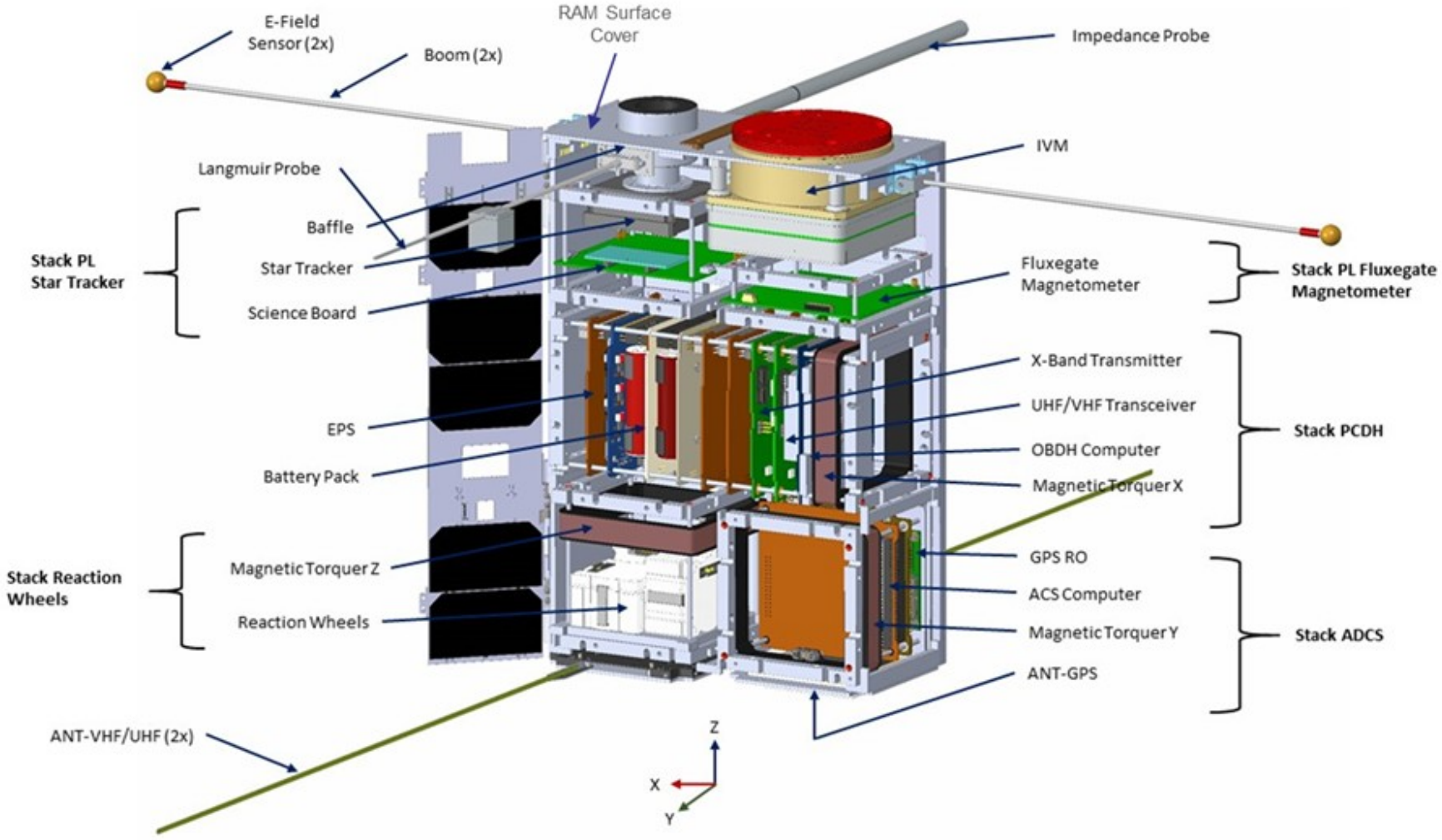

Figure 1: SPORT Spacecraft System Overview

Table 1: SPORT Science Measurement and Spacecraft System Requirements from the Science Traceability Matrix (STM)

The Scintillation Prediction Observation Research Task (SPORT)		Instrumentation	Spacecraft
Observational Approach	**Science Measurement Requirements**	**Instrument Approach**	**Space Systems Requirements**
1) What is the state of the ionosphere that gives rise to the growth of plasma irregularities that extend into and above the F-peak?			
Observations in the 1700 to 0100 LT sector over -30° to 30° latitude Height profiles of the plasma density to specify the magnitude and height of the F peak density in the EA Vertical ion drifts at or below the F peak in the EA	**Plasma Density Profile** 1) 140 to 450 km alt 2) 10^4 to 10^7 p/cm^3 range 3) 20% p/cm^3 accuracy 4) 1000 km along track sampling **Ion Drifts (Earth Reference Frame)** 1) ±800 m/s Range 2) 20 m/s precision & accuracy 3) 10 km along track sampling	**GPS Occultation** Observe GPS satellite occultation along and to the sides of the orbit plane to obtain line of site TEC **Ion Velocity Meter** Observe vertical ion drifts by angle of arrival of heavy ions at detector	**Satellite Orbit** 1) ≥1 year mission life 2) 40° to 55° inclination 3) 350 to 450 km altitude 4) ±10 km eccentricity **Spacecraft** 1) ± 5° Ram Pointing 1σ 2) ≤1 km position knowledge 3) ≤10 ms timing
2) How are plasma irregularities at satellite altitudes related to the radio scintillations observed passing through these regions?			
Observations in the 2200 to 0200 LT sector over -30° to 30° latitude Observations of irregularities in electron density and E-field power spectral density in slope from 200 km to 200 m	**E-Field (Earth Reference Frame)** 1) ±45 mV/m range 2) 1.1 mV/m precision & accuracy 3) 1 km along track sampling 4) 10 km - 200 m along track waves **Plasma Density** 1) 10^3 to 10^7 p/cm^3 range 2) 10^3 p/cm^3 precision & accuracy 3) 1 km along track sampling 4) 10 km - 200 m along track waves **B-field** 1) ± 56,000 nT range 2) ±100 nT precision and accuracy 3) 1 km along track sampling	**E-Field Double Probe** Observe probe floating potential for AC E-fields from irregularity **GPS Occultation** S4 scintillation index **Langmuir/Impedance** Observe DC and AC probe response for relative and absolute electron density and observe irregularities **Three Axis Magnetometer** Support VxB computation for ion velocity and E-Field measurements	**Spacecraft Mechanisms** 1) ≥0.6 m tip-to-tip booms **Attitude** **(Post Flight Knowledge)** 1) ≤ 0.05° 1σ-uncertainty

Content (sTEC), but for brevity, this will be shortened to TEC. SPORT will make use of CTECS to obtain electron density profiles at low latitudes and to detect the presence of scintillation

Ion Velocity Meter (IVM)

The UTD provided Ion Velocity Meter (IVM) is mounted on the spacecraft to view along the velocity vector in the ram direction, and acts as two traditional instruments. The first function is a planar retarding potential analyzer (RPA), which determines the energy distribution of the thermal plasma along the sensor look direction. The second is a planar ion drift meter (IDM), which measures arrival angle of the thermal plasma with respect to the look direction in two mutually perpendicular planes approximately in the local vertical. and the local horizontal. Internal grids are biased to reject the collection of thermal electrons and to control the energy of incident ions that have access to the collector. The incident arrival angle of the ions is derived from the ratio of currents to a segmented collector. The IVM is used to collect data sets to determine the Vector Ion Drift, Total Ion Density, Ion Temperature, and the O+/H+ Relative Composition

Miniature Science Magnetometer (MSM)

A GSFC-produced miniature vector magnetometer system will provide high-resolution measurements of the ambient magnetic field with sufficient sensitivity to potentially observe perturbations due to pressure gradients, diamagnetic cavities, or Alfvenic waves. The fluxgate magnetometer is deployed on a relatively short boom (~20 cm) to remove it from the majority of the magnetic noise of the spacecraft bus.

SPACECRAFT SYSTEMS TO SUPPORT SCIENCE CONOPS

The ancillary spacecraft data, specified in Table 2 are required for SPORT science data processing. These values are collected and updated using automatic software tools at the EMBRACE facility over the duration of the mission.

The Ancillary files utilize the NetCDF format using 1-second cadence per record. The unique identifier is `T0` found in field #1. The following fields in the Ancillary data files are described as follows.

Parameters 1 through 3:

The first three parameters are provided by the SPORT flight computer clock, which is regularly updated using information from the `BESTXYZ` frame header from the CTECS instrument's Novatel receiver, documented on the Novatel datasheet on Section 3.2.17 [*Novatel, 2000*]. `T0` is the GPS time in number of milliseconds since 00:00.0001 on Jan 6, 1980. The GPS reference week number (`GPS-Week`) incorporates 2 bytes to accommodate the 10-bit value [*Novatel, 2000*]. `GPS-Week-Time` is the number of milliseconds from the beginning of the GPS reference week (4 bytes).

Parameters 4 through 8:

Note that `T0` does not contain leap seconds. However, Coordinated Universal Time (`UTC`) used in the SPORT Ancillary Data files do incorporate leap seconds, which as of CY2021, adds 18 seconds to the GPS time `T0` [*Sullivan et al., 2016*]. All `UTC` parameters will be calculated on ground at EMBRACE, and they will be based on the GPS reference week number and milliseconds from the beginning of that GPS reference week.

Parameters 9 through 14:

The spacecraft position and velocity data are provided in the `BESTXYZ` data frames from CTECS instrument [*Novatel, 2000*] in the Earth-Centered Earth-Fixed (ECEF) Cartesian coordinate system (e.g., *Cai et al., 2011*). ECEF is a geocentric, non-inertial coordinate system, defined by a z-axis aligned with the minor axis of the ellipsoid that represents the surface of the oblate Earth, an x-axis defined by the vector from the Earth's center of mass to the intersection of the Prime Meridian with the oblate Earth's equator, and a y-axis that completes the right-hand coordinate system (Figure 2).

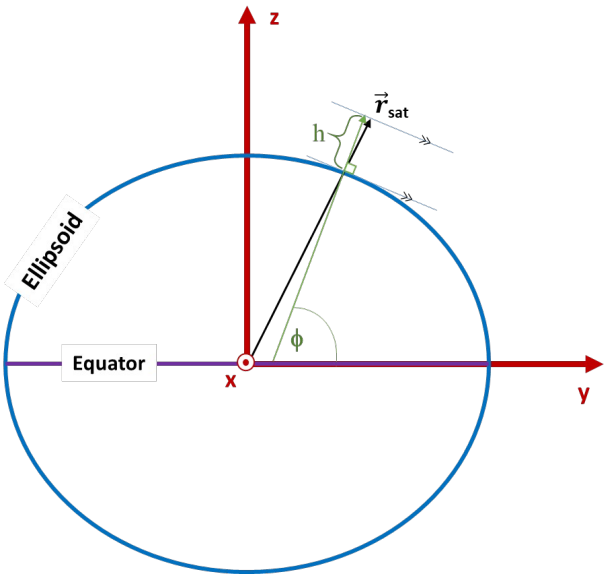

Figure 2: WGS84 Coordinate System, an ECEF coordinate system, depicting latitude and altitude for ellipsoid

Table 2: Spacecraft Data Fields

#	Variable	Type	Units	Description
1	T0	Double	ms	GPS Time in milliseconds since 00:00 Jan6, 1980
2	GPS-Week	Integer	Weeks	GPS week (1-1023)(2 Bytes)
3	GPS-Week-Time	Double	ms	Milliseconds since start of GPS Week
4	UTC-Year	Integer	Years	UTC - Year
5	UTC-Month	Integer	Months	UTC - Month
6	UTC-Day	Integer	Days	UTC – Day of Month
7	UTC	Double	Hours	UTC – Time of Day (Decimal hours to ms precision)
8	UTC-DOY	Integer	Days	UTC - Day of the Year
9	SC_Vx_GPS	Double	km/s	Spacecraft Velocity, x axis (ECEF)
10	SC_Vy_GPS	Double	km/s	Spacecraft Velocity, y axis (ECEF)
11	SC_Vz_GPS	Double	km/s	Spacecraft Velocity, z axis (ECEF)
12	SC_X_GPS	Double	km	Spacecraft Position, x axis (ECEF)
13	SC_Y_GPS	Double	km	Spacecraft Position, y axis (ECEF)
14	SC_Z_GPS	Double	km	Spacecraft Position, z axis (ECEF)
15	SC_Vx	Float	km/s	Spacecraft Velocity, x axis (ECI, J2000)
16	SC_Vy	Float	km/s	Spacecraft Velocity, y axis (ECI, J2000)
17	SC_Vz	Float	km/s	Spacecraft Velocity, z axis (ECI, J2000)
18	SC_X	Float	km	Spacecraft Position, x axis (ECI, J2000)
19	SC_Y	Float	km	Spacecraft Position, y axis (ECI, J2000)
20	SC_Z	Float	km	Spacecraft Position, z axis (ECI, J2000)
21	SC_Lat	Float	Degrees	Spacecraft Geodetic Latitude, (WGS 84)
22	SC_Long	Float	Degrees	Spacecraft Geodetic Longitude, (WGS 84)
23	SC_Alt	Float	km	Spacecraft Geodetic Altitude (WGS 84)
24	SC_ZROT	Float	Degrees	Euler rotation about z-axis (QSW)
25	SC_XROT	Float	Degrees	Euler rotation about x-axis (QSW)
26	SC_YROT	Float	Degrees	Euler rotation about y-axis (QSW)
27	SZA	Float	Degrees	Solar Zenith Angle
28	SLT	Float	Hours	Solar Local Time
29	SC_SUN_ANGLE	3 × Float	Unitless	S/C-Sun Unit vector projected onto ADCS S/C Coords
30	MLT_QD	Float	Hours	Magnetic Local Time (QD)
31	LAT_QD	Float	Degrees	Magnetic Latitude (QD)
32	LONG_QD	Float	Degrees	Magnetic Longitude (QD)
33	APEX_QD	Float	km	Magnetic Flux Tube Apex Height (QD)
34	MTORQ_ACTIV_X	Byte	Logic	Magnetic Torque Bar Activation Flag, x axis
35	MTORQ_ACTIV_Y	Byte	Logic	Magnetic Torque Bar Activation Flag, y axis
36	MTORQ_ACTIV_Z	Byte	Logic	Magnetic Torque Bar Activation Flag, z axis
37	EPHEM_PROP	Byte	Logic	Ephemeris Flag Propagated (Interp/Extrap?)
38	ATT_PROP	Byte	Logic	Attitude Flag Propagated (Interp/Extrap?)
39	STAR_TRACK	Byte	Logic	Star Tracker Flag Used (v. Not Used) in ATT determ.
40	MAX_SLRPNL_V	Float	Volts	Maximum Solar Panel Voltage
41	MAX_SLRPNL_I	Float	Amps	Maximum Solar Panel Current
42	TLM_QUAL	Integer	logic	Relevant Telemetry Valid Flags (TBD)
43	B_Vec	3 × Float	nT	3-component Magetic Field (model) vector in S/C frame
44	SC_ENU_XFORM	9 × Float	radians	3x3 S/C frame to ENU Transformation Matrix

Parameters 15 through 20:

On the ground, EMBRACE calculates the spacecraft position and velocity in the Earth Centered Inertial (ECI) coordinate system using the data collected by the S/C and supplemented by model data from the SGP4 propagator [*Vallado and Crawford, 2008*]. This transforms the position and velocity vectors into the inertial Earth-Centered Inertial (ECI/J2000) geodetic cartesan coordinates [e.g., *Kumar, 1995*], defined by the x-axis aligned with the Earth's vernal equinox line, the z-axis aligned with the Earth's rotation axis, and the y-axis completing the right-hand coordinate system.

Parameters 21 through 23

The S/C position data in the Cartesian ECEF coordinate system (i.e., Parameters 12 through 14) are calculated based on the non-inertial World Geodetic System (WGS84) datum that describes the shape of the Earth as an ellipsoid (i.e., an oblate Earth). Parameters 21 through 23 are the values of the S/C position in spherical coordinates; that is, as represented by latitude, longitude, and altitude in ECEF according to the WGS84 datum [e.g., *Kumar, 1984*]. The WGS84 datum provides the most accurate approximation of fitting a single ellipsoid to the surface of the Earth [e.g., *Lohmar, 1988*], and is still the standard in use today by GPS receivers to provide latitude, longitude, and altitude solutions. The WGS84 ellipsoid is specified as having a semi-major axis of 6378.137 km at the equator and a semi-minor axis of 6356.752 km at the poles, corresponding to a flattening factor of 1/298.257223 [Table 3.5 in *NGA, 2014*]. A graphical depiction of the WGS84 Coordinate System latitude and altitude appears in Figure 2. The geometric center of the WGS84 Ellipsoid serves as the origin of WGS84 Coordinate System. The x-y plane is defined by the great circle circumscribed about the semi-major axis of the ellipsoid (i.e., the equatorial plane). The z-axis is normal to this plane and passes through the ellipsoid's center of mass; it thus serves as the rotational axis of the ellipsoid. The x-axis points from the origin to the International Reference Meridian (IRM) projected onto the equatorial plane. (The IRM is approximately 5.3 arcseconds offset from the Prime Meridian at the latitude of the Royal Observatory in Greenwich, UK [*Malys et al., 2015*].) The y-axis completes the right-hand coordinate system. In that case, the WGS84 longitude of the S/C position is defined as the angle λ between the IRM and the position vector projected onto the x-y plane.

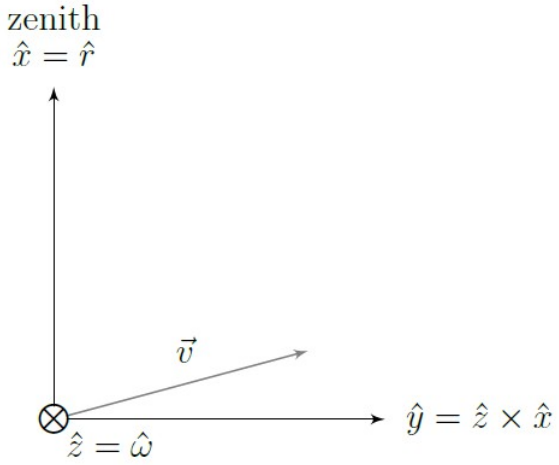

Figure 3: QSW Orbit Coordinate Frame

Parameters 24 through 26:

The spacecraft attitude knowledge data are provided relative to the basis vectors in the QSW orbit frame at any given time. The QSW orbit coordinate frame is depicted in Figure 3. Given the S/C position $\vec{r}$, velocity $\vec{v}$ and its mass-specific angular momentum $\vec{\omega} = \vec{r} \times \vec{v}$ in the J2000 reference system, then the QSW local orbital frame is defined here as: $\hat{x} = \vec{r}/|\vec{r}|$; $\hat{z} = \vec{\square}/|\vec{\square}|$; and $\hat{y} = \hat{z} \times \hat{x}$.

Note that in this simplified representation of the QSW frame, the symbol ⊗ indicates a vector perpendicular to the plane pointing into page. As the SC velocity $\vec{v}$ is orthogonal to $\vec{z}$, then it is in the xy plane. Normally $\vec{v}$ will be very close to the $\hat{y}$ direction and exactly in the $\hat{y}$ direction if the S/C is in a circular orbit.

Transforming QSW coordinates to S/C coordinates is accomplished by successive application of matrix rotations. The S/C body coordinates are then given by multiplying the rotation matrices about each of the three axes, defined as follows:

$$R_z(\alpha) = \begin{bmatrix} \cos\alpha & \sin\alpha & 0 \\ -\sin\alpha & \cos\alpha & 0 \\ 0 & 0 & 1 \end{bmatrix};$$

$$R_y(\beta) = \begin{bmatrix} \cos\beta & 0 & -\sin\beta \\ 0 & 1 & 0 \\ \sin\beta & 0 & \cos\beta \end{bmatrix};$$

$$R_x(\gamma) = \begin{bmatrix} 1 & 0 & 0 \\ 0 & \cos\gamma & \sin\gamma \\ 0 & -\sin\gamma & \cos\gamma \end{bmatrix}$$

Thus, the total rotation matrix is given by:

$$R = R_z(\alpha)R_y(\beta)R_x(\gamma)$$

Here, Parameters 24 through 26 represent α, β, and ɣ as the rotational angles about the z, y, and x-axes, respectively.

Parameters 27 through 29

The Solar Zenith Angle (SZA), Parameter 27, is defined as follows. In Figure 4Error: Reference source not found, S, T and C are the center of: mass of the Sun, Earth, and spacecraft, respectively. These three points define a plane. The angle α between the spacecraft's zenith, C and S is the Solar Zenith Angle. From Figure 4, $\alpha = \xi + \zeta$. Note that $\overline{TC} \ll \overline{TS}$, so that $\zeta \approx 0$ and $\xi \approx \alpha$.

Parameter 28, the Solar Local Time (SLT), is simply the geocentric longitude converted from degrees to hours (i.e., 15 degrees of longitude per hour of time) and added to the UTC decimal hours. Finally, Parameter 29 quantifies the unit vector of the satellite-Sun line projected onto the S/C coordinate frame axes (Figure 7) as the sum of fractional values of $\hat{x}_{S/C}$, $\hat{y}_{S/C}$, and $\hat{z}_{S/C}$.

Parameters 30 through 33:

These four parameters correspond to the Magnetic Local Time (MLT), latitude, longitude, and apex height in the Quasi-Dipole (QD) coordinate system, which is one of two Magnetic Apex coordinate systems described in *Laundal and Richmond (2017)*. The QD coordinate system is different from the others described here in that it is non-orthogonal, meaning that coordinate transformations from other systems to the

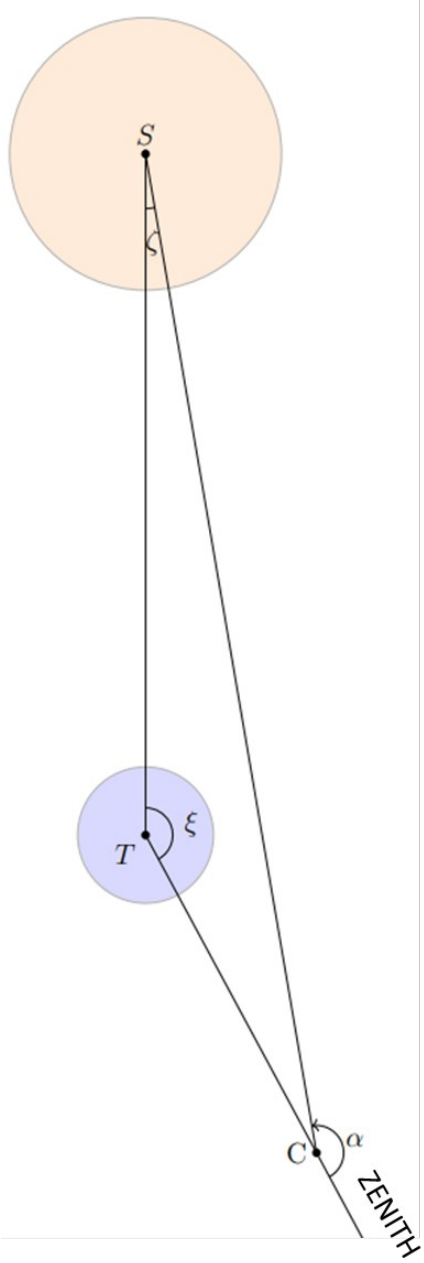

Figure 4: Sun-Satellite Geometry

QD system cannot be accomplished using simple transform matrix multiplication. These four parameters are calculated at the EMBRACE facility using software that traces the Earth's magnetic field line from the satellite's position to the highest point above the surface of the Earth – i.e., the apex of the field line. The Earth is assumed to be oblate, and the magnetic field model is the IGRF-13 [*Alken et al., 2021a*]. By definition, the satellite's altitude in the QD coordinate system is equal to that in the ECI coordinate system, and thus it is not duplicated with this set. See [*Laundal and Richmond,*

2017] for a complete description of the QD and other geomagnetic coordinate systems that may be of interest.

Parameters 34 through 36:

These three Parameters describe the three Magneto-torquer Flags (one per axis in the s/c reference frame) that are high when the magneto-torquers are active and low when they are not. These will be computed on ground for each coil duty cycle provided by the ADCS telemetry frame.

Parameters 37 through 39:

The flag `EPHEM_PROP` is in the high state when the satellite position data are based on calculations using orbit propagators driven by two-line element (TLE) sets from a non-SPORT data source (e.g., *SpaceTrack*). The flag `ATT_PROP` is in the high state when the satellite attitude data are based on calculations using rate data and modeling tools. The `STAR_TRACK` flag is in the high state when the SPORT Star Tracker data were used in the calculation of the S/C attitude data.

Parameters 40 and 41:

The spacecraft EPS (Energy and Power Supply) system provides maximum Solar Panel Voltage and maximum Solar Panel Current, in the EPS housekeeping data packet called DD_HOU_EPS_2. The solar panel voltages is provided by the BCR[X] voltage TM and each BCR has two input channels, where the current is provided on BCR[X] Currents TM. The BCR utilization is organized according to Figure 5.

Parameter 42:

TLM valid flags in integer form.

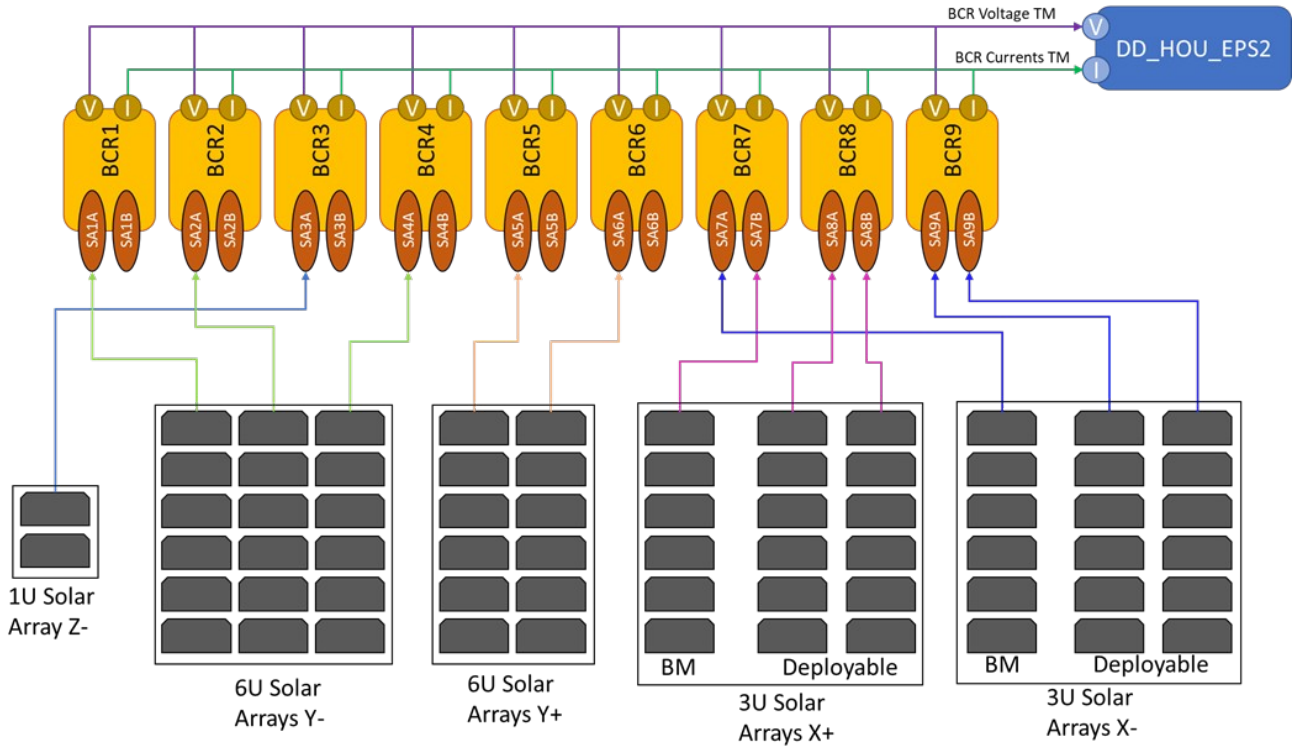

Figure 5: SPORT Solar array configuration and BCR utilization on EPS.

Parameter 43:

`B_vec` is the three-component magnetic field from the thirteenth generation of the International Geophysical Reference Field (IGRF-13) model [*Alken et al., 2021b*] in the S/C frame of reference (i.e., in the S/C coordinate frame, shown in Figure 6). This parameter is calculated at the EMBRACE facility by retrieving the magnetic field components from IGRF-13 as a function of S/C position (in WGS84) and using the orientation of the S/C reference axes in East-North-Up (ENU) to map those components to the S/C coordinate frame.

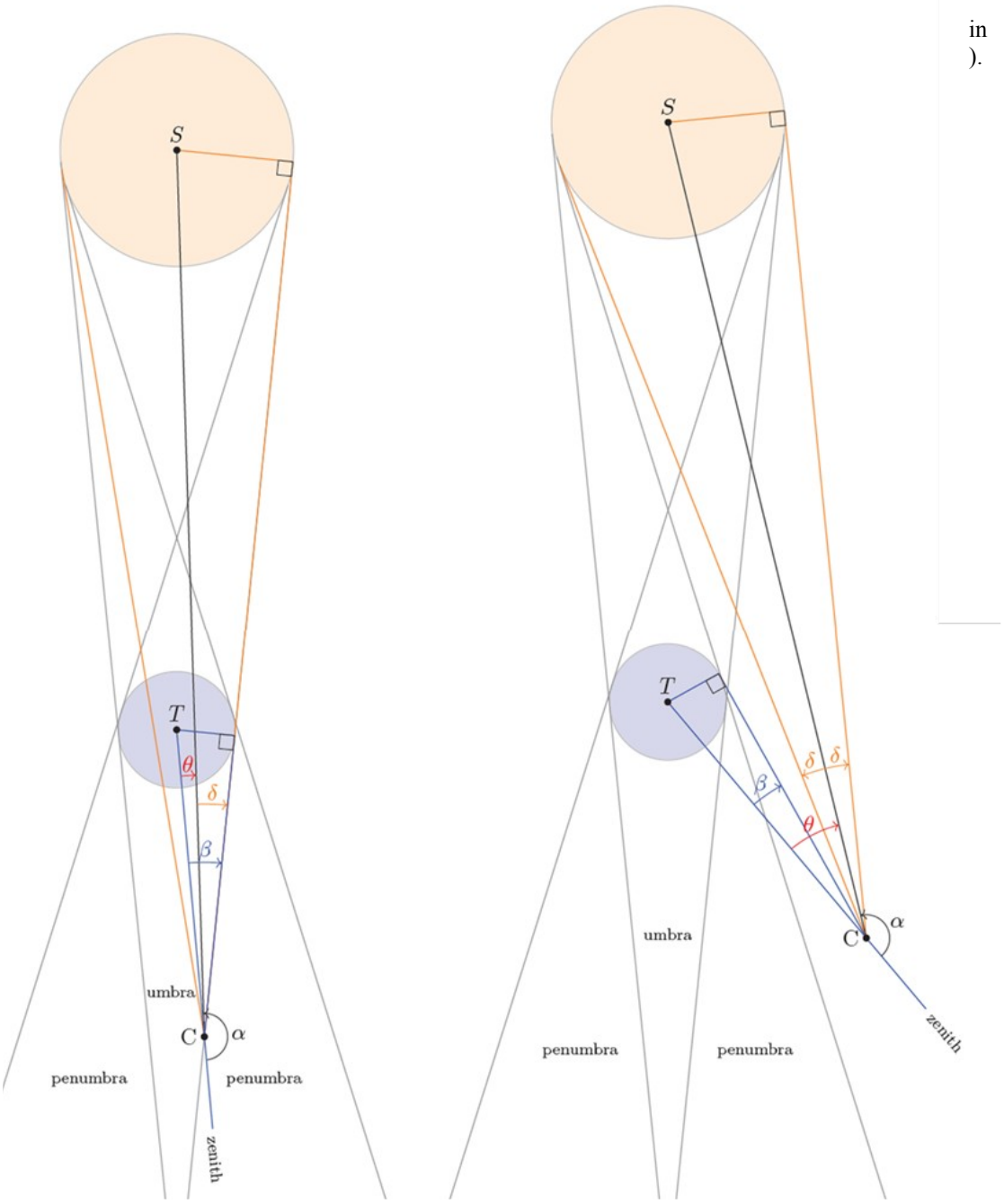

Figure 6: Depicted are the Sun (orange), Earth (gray), and SPORT satellite (at Point C), showing the satellite at the edge between the umbra and penumbra (left) and in full sunlight (right).

Parameters 44 through 46:

These three parameters are nine-element rotation matrices to transform vector-based quantities from one coordinate system to another. Parameter 44 data contain the transformation matrices to convert from the local S/C coordinate system to the local geodetic ENU coordinate system. Parameter 45 data contain the transformation matrices for converting from the S/C coordinate system to the global geodetic ECI/J2000. Parameter 46 data contain the transformation matrices for converting from the ECEF to the global geodetic ECI/J2000. These transformation matrices are calculated by EMBRACE.

Parameter 47 and 48:

Parameter 47 gives the Earth's rotation velocity at the S/C altitude mapped onto the S/C coordinate frame, with axes defined in **Figure 7**Error: Reference source not found. Parameter 48 represents the S/C velocity (relative to the center of the Earth) in the S/C reference frame and is quantified by the sum of fractional values of $\hat{x}_{S/C}$, $\hat{y}_{S/C}$, and $\hat{z}_{S/C}$.

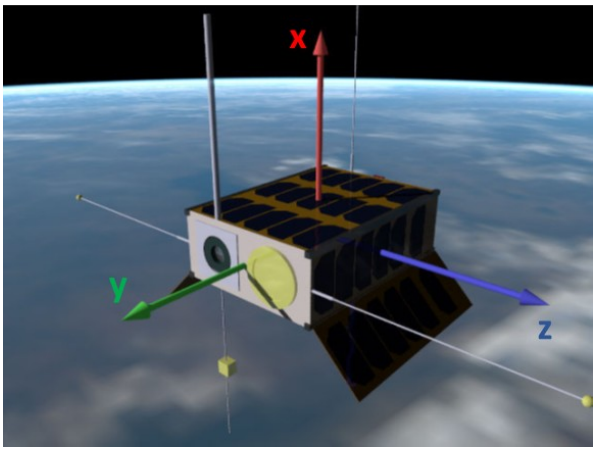

Figure 7: S/C Coordinate Frame used for ADCS and GNC parameters. Note that axis definitions differ from the mechanical coordinate system in Figure 1.

Parameter 49:

This parameter describes the eclipse state of the S/C in integer form, where no eclipse = 0, full eclipse (umbra) = 1, and partial eclipse (penumbra) = 2. The umbra and penumbra geometry is depicted in **Figure 6**Error: Reference source not found. Recall S, T and C are the center of mass of the Sun, Earth, and spacecraft, respectively. The gray lines are tangent to the surfaces of the Sun and Earth. These lines behind the Earth define the umbra and penumbra regions. Figure 6 shows the geometry of the satellite at the edge of the Earth's umbra/penumbra (left) and in full sunlight (right). Recall the angle between the spacecraft zenith, C and S is the SZA α. The supplementary angle of the SZA is the angle $\theta = \pi - \alpha$. The half-apex angle of the cone defined by the solar surface and apex at point C is given by $\delta = \sin^{-1}(R_s/d_s)$, where R_S is the radius of the Sun and d_S is the distance between C and S. Similarly, $\beta = \sin^{-1}(R_T/d_T)$, where R_T is the radius of the Earth and d_T is the distance between C and T. Then we have three eclipse conditions defined as follows: 1) C is outside the umbra and penumbra if $\theta > \beta + \delta$; 2) C is inside the umbra if $\theta + \delta \leq \beta$; and 3) C is inside the penumbra otherwise.

DATA ACCESS

The EMBRACE program is based on open source data policy. It is structured to run a network of sensors on the ground and has already included initiatives involving space-based instruments through cooperative engagements. For example, EMBRACE cooperated with NOAA to provide a downlink system for COSMIC 2. The SPORT data processed and disseminated by EMBRACE will continue this open source policy.

SPORT S/C Science Data are actually stored at two facilities: EMBRACE and NASA GSFC's Space Physics Data Facility (SPDF). Only Levels 2 and 3 data products will be archived at GSFC. As the GSFC site is considered to be a mirror archive site, the majority of the information in this Section is focused on the EMBRACE facilities.

The EMBRACE web-site is organized to offer a clear communication with users. It prompts the activity indices of the space weather environment in the first page. It offers graphical user interface to visualize and obtain the data. It is open to innovation with infrastructure of computation for new ideas on dealing with data and models for users that want to collaborate.

CONCLUSION

The SPORT 6U CubeSat mission is instrumented with a set of space environment sensors that provides a rich set of ionospheric data tailored to the investigation of equatorial plasma bubbles (EPBs) and associated ionospheric scintillation of GPS signals. The detailed parameters listed in this paper make it possible to conduct research on large-scale EPBs when combined with other measurements from ground- and space-based observatories. In addition to the improvement of ionospheric EPB statistical occurrence models, specifically with respect to longitudinal effects, coordinated campaigns for enhanced science return will be conducted within the broader space weather community.

ACKNOWLEDGMENTS

The Authors would like to thank NASA Science Mission Directorate, SOUTHCOM, and the Brazilian Government for funding the SPORT Mission.

REFERENCES

Alken, P., Thébault, E., Beggan, C.D. et al. International Geomagnetic Reference Field: the thirteenth generation. Earth Planets Space 73, 49 (2021a).

Alken, Patrick, Erwan Thebault, C. D. Beggan, Julien Aubert, Julien Baerenzung, William J. Brown, S. Califf et al. "Evaluation of candidate models for the 13th generation International Geomagnetic Reference Field." Earth, Planets and Space 73, no. 1 (2021b): 1-21.

CCSDS, Report Concerning Space Data System Standards, Navigation Data – Definitions and Conventions, CCSDS Green Book 500.0-G-4, 2019.

Cai, Guowei, Ben M. Chen, and Tong Heng Lee. "Coordinate systems and transformations." In Unmanned rotorcraft systems, pp. 23-34. Springer, London, 2011.

Drake, Samuel Picton. "Converting GPS coordinates [phi, lambda, h] to navigation coordinates (ENU)." (2002).

Klobuchar, 1987, Ionospheric time-delay algorithm for single-frequency GPS users, IEEE Transactions on Aerospace and Electronic Systems, p325-331

Kumar, Muneendra. "World geodetic system 1984: A modern and accurate global reference frame." Marine Geodesy 12, no. 2 (1988): 117-126.

Kumar, M. U. N. E. E. N. D. R. A. "Coordinate Frames.", Sections II and III, AGARDOGRAPH AGARD AG (1995): 7-7.

Lehtinen, Mikko, Ari Happonen, and Jouni Ikonen. "Accuracy and time to first fix using consumer-grade GPS receivers." In *2008 16th International Conference on Software, Telecommunications and Computer Networks*, pp. 334-340. IEEE, 2008.

Laundal, Karl Magnus, and Arthur D. Richmond. "Magnetic coordinate systems." Space Science Reviews 206, no. 1-4 (2017): 27-59.

Lohmar, Franz Josef. "World Geodetic System 1984—Geodetic Reference System of GPS Orbits." In GPS-Techniques Applied to Geodesy and Surveying, pp. 476-486. Springer, Berlin, Heidelberg, 1988.

Malys, Stephen, John H. Seago, Nikolaos K. Pavlis, P. Kenneth Seidelmann, and George H. Kaplan. "Why the Greenwich meridian moved." Journal of Geodesy 89, no. 12 (2015): 1263-1272.

Mannucci, A. J., B. T. Tsurutani, O. Verkhoglyadova, A. Komjathy, and X. Pi. "Use of radio occultation to probe the high-latitude ionosphere." Atmospheric Measurement Techniques 8, no. 7 (2015): 2789-2800.

NGA, National Geospatial-Intelligence Agency (NGA) Standardization Document Department Of Defense World Geodetic System 1984, NGA.STND.0036_1.0.0_WGS84, 2014.

Novatel OEM6® Family Firmware Reference Manual, 2000, link last accessed July 28, 2021: https://hexagondownloads.blob.core.windows.net/public/Novatel/assets/Documents/Manuals/om-20000129/om-20000129.pdf

Rickman, Steven L. "Introduction to On-orbit thermal environments," in Thermal and Fluids Analysis Workshop, 2014.

Sullivan, John P., Matthew Robert Carver, and Benjamin Norman. Contents of GPS Data Files. No. LA-UR-16-29314. Los Alamos National Lab. (LANL), Los Alamos, NM (United States), 2016.

Vallado, David, and Paul Crawford. "SGP4 orbit determination." In AIAA/AAS Astrodynamics Specialist Conference and Exhibit, p. 6770. 2008.